Crystal structure of terazosin hydrochloride dihydrate (Hytrin®), $C_{19}H_{26}N_5O_4Cl(H_2O)_2$

Austin M. Wheatley,[1] James A. Kaduk,[1,2,a)] Martin Vickers,[3] Amy M. Gindhart,[4] Joseph G. Sunzeri,[4] and Thomas N. Blanton[4]
[1]*North Central College, 131 S. Loomis St., Naperville, Illinois 60540*
[2]*Illinois Institute of Technology, 3101 S. Dearborn St., Chicago, Illinois 60616*
[3]*Department of Chemistry, University College London, 20 Gordon St., London WC1H 0AJ, UK*
[4]*ICDD, 12 Campus Blvd., Newtown Square, Pennsylvania 19073-3273*

(Received 2 February 2018; accepted 17 May 2018)

The crystal structure of terazosin hydrochloride dihydrate has been solved and refined using synchrotron X-ray powder diffraction data, and optimized using density functional techniques. Terazosin hydrochloride dihydrate crystallizes in space group *P-1* (#2) with $a = 10.01402(4)$, $b = 10.89995(4)$, $c = 11.85357(4)$ Å, $\alpha = 89.5030(3)$, $\beta = 71.8503(3)$, $\gamma = 66.5632(2)°$, $V = 1118.143(8)$ Å^3, and $Z = 2$. The terazosin cation occurs in an extended conformation. The crystal structure is dominated by hydrogen bonds. The most notable are the O–H• • • Cl from the water molecules to the chloride anion and N–H• • • Cl from the protonated ring nitrogen to the chloride. The amino group donates protons to each of the two water molecules. The powder pattern has been submitted to ICDD® for inclusion in the Powder Diffraction File™. © *2018 International Centre for Diffraction Data.*
[doi:10.1017/S0885715618000490]

Key words: terazosin hydrochloride dihydrate, Hytrin®, powder diffraction, Rietveld refinement, density functional theory

I. INTRODUCTION

Terazosin hydrochloride dihydrate (brand name Hytrin®) is an α-adrenergic blocker used to treat hypertension or to improve urination in males with benign prostatic hyperplasia. The IUPAC name (CAS Registry number 70024-40-7) is [4-(4-amino-6,7-dimethoxyquinazolin-2-yl)piperazin-1-yl]-(oxolan-2-yl)methanone dihydrate hydrochloride. A two-dimensional molecular diagram is shown in Figure 1.

Crystalline terazosin hydrochloride dihydrate is disclosed and claimed in US Patent 4 251 532 (Roteman, 1979; Abbott Laboratories, Abbott Park, IL, USA). The text of this patent indicates that it contains diffraction patterns in Figures 1 and 2, but these figures are DSC curves. X-ray powder patterns of "the prior art dihydrate form" of terazosin are contained in several other Abbott patents, notably US Patent 5 294 615 (Meyer and Bauer, 1994).

This work was carried out as part of a project (Kaduk *et al.*, 2014) to determine the crystal structures of large-volume commercial pharmaceuticals, and include high-quality powder diffraction data for these pharmaceuticals in the Powder Diffraction File (Fawcett *et al.*, 2017).

II. EXPERIMENTAL

The contents (powder) of a terazosin 5 mg capsule (Sandoz Inc., Holzkirchen, Germany) were removed from the gelatin case then front packed into a standard sample holder. The X-ray powder diffraction pattern was measured on a Bruker D2 Phaser diffractometer using Cu$K\alpha$ radiation (5–70°2θ, 0.0202144° steps, 0.5 s step^{-1}, 0.6° divergence slit, 2.5° Soller slits, 3 mm scatter screen height). The major phase was α-lactose monohydrate (Figure 2). The peaks from the minor phase(s) did not match either of the two PDF entries for terazosin hydrochloride dihydrate, or that of anhydrous material from US Patent 5 856 482 (Cannata *et al.*, 1999). The peak intensities of the terazosin hydrochloride dihydrate entries in the Powder Diffraction File (PDF®) (ICDD, 2017) patterns differ, indicating that one or both of them might exhibit preferred orientation (Figure 3). PDF entry 00-047-2073 is a low-precision "blank" pattern, but 00-060-1210 is a high-quality "star" pattern. Unit-cell and connectivity searches in the Cambridge Structural Database (Groom *et al.*, 2016) did not yield any crystal structures of terazosin derivatives.

The pattern of PDF entry 00-060-1210 was measured using Cu$K\alpha_1$ radiation and was indexed on a primitive triclinic unit cell with $a = 10.893(1)$, $b = 11.845(1)$, $c = 10.005(1)$ Å, $\alpha = 108.232(3)$, $\beta = 113.451(2)$, $\gamma = 89.442(3)°$, $V = 1115.04$ Å^3, and $Z = 2$. The reported cell was converted to the reduced cell using a tool in the PDF database. The terazosin cation was built in Spartan '16 (Wavefunction, 2017) and the minimum energy conformation was determined. The molecule was saved as a .mol2 file and converted into a Fenske-Hall Z-Matrix using OpenBabel (O'Boyle *et al.*, 2011).

The structure solution using the experimental PD3 pattern from entry 00-060-1210 was difficult, which we believe to be the result of preferred orientation (the refined texture index was 1.383). What ultimately seems to have been successful was to use terazosin, Cl, and 2O as fragments in FOX

a)Author to whom correspondence should be addressed. Electronic mail: kaduk@polycrystallography.com

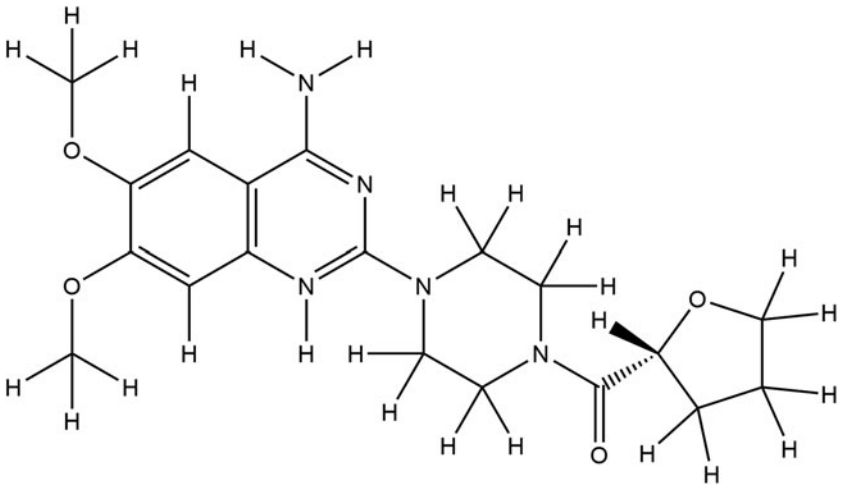

Figure 1. The molecular structure of the terazosin cation.

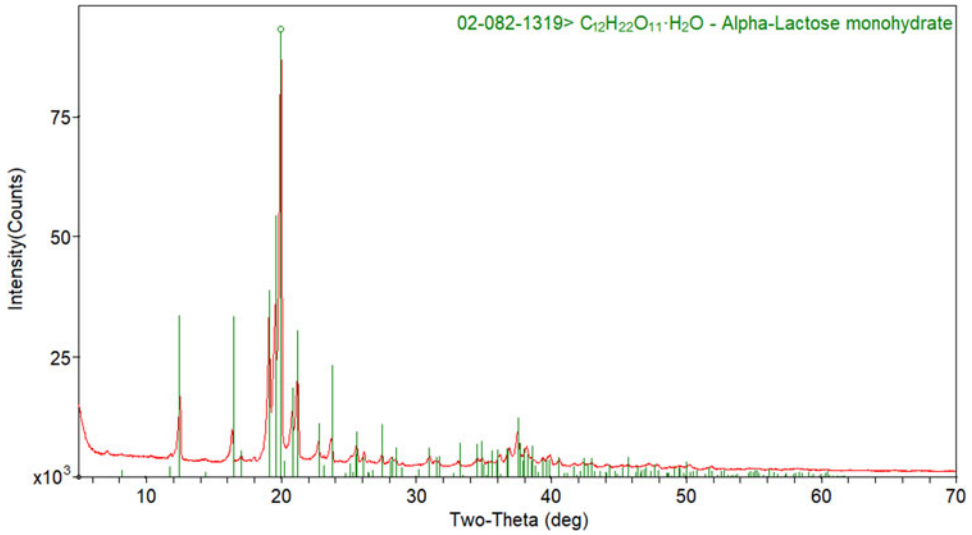

Figure 2. (Color online) X-ray powder diffraction pattern of powder removed from a terazosin 5 mg capsule, showing that the major phase is α-lactose monohydrate.

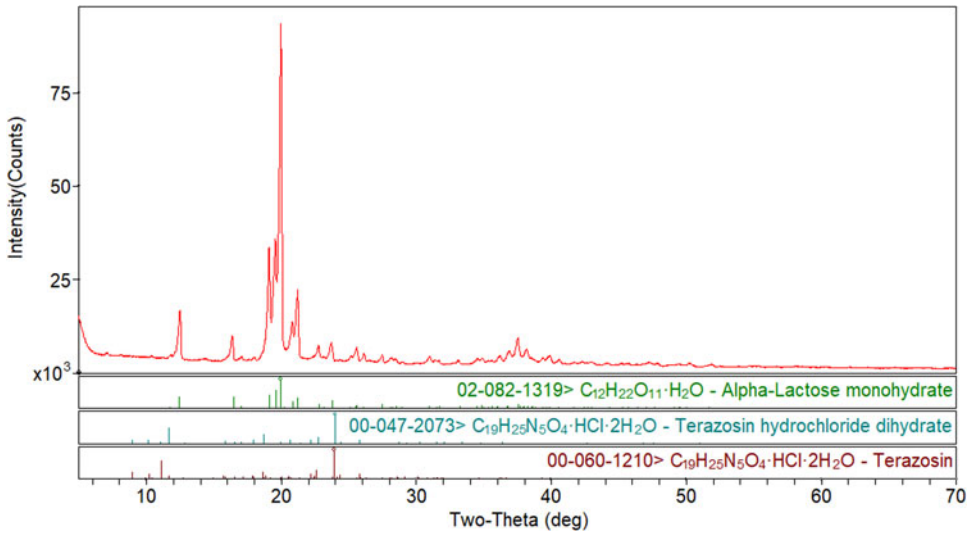

Figure 3. (Color online) X-ray powder diffraction pattern of powder removed from a terazosin 5 mg capsule, compared with the two PDF entries for terazosin hydrochloride dihydrate and α-lactose monohydrate. The relative intensities in the two terazosin hydrochloride dihydrate database patterns differ, indicating that one or both of the patterns may suffer from preferred orientation.

https://doi.org/10.1017/S0885715618000490 Published online by Cambridge University Press

(Favre-Nicolin and Černý, 2002). Included in the solution process were variation of the March–Dollase ratio and the direction of the preferred orientation. A reasonable hydrogen bonding pattern appeared, but on refinement one of the water molecules moved too close to the ketone group (O• • • O = 1.89 Å). There was a void in the structure at 00½, which was filled with a water molecule. The water–ketone distance became much more reasonable. The compound appeared to be a hemipentahydrate. Although the refinement yielded plausible residuals (R_{wp} = 0.1287, R_p = 0.0966, χ^2 = 54.17) (Figure 4), some features of the structure seemed to be chemically unusual. The C_4N_2 ring was in a boat conformation, and a Mogul geometry check (Bruno *et al*., 2004; Sykes *et al*., 2011) showed that the tetrahydrofuran ring was in an unusual conformation. We felt that more accurate characterization required a better data set, so a synchrotron powder pattern was obtained.

Terazosin hydrochloride dihydrate was a commercial reagent, purchased from USP (Lot #G0F290), and was used as-received. The white powder was packed into a 1.5 mm diameter Kapton capillary, and rotated during the measurement at ~50 cycles s^{-1}. The powder pattern was measured at 295 K at beam line 11-BM (Lee *et al*., 2008; Wang *et al*., 2008) of the Advanced Photon Source at Argonne National Laboratory using a wavelength of 0.457667 Å from 0.5 to 50°2θ with a step size of 0.001° and a counting time of 0.1 s $step^{-1}$.

The initial refinement used the known unit cell, the previous structural model, and the 2–26° portion of the diffraction pattern (d_{min} = 1.017 Å), but was not completely satisfactory (reduced χ^2 = 4.59). The structure was re-solved using the synchrotron data with FOX ($\sin\theta/\lambda_{max}$ = 0.3 $Å^{-1}$). A terazosin cation, a chlorine atom, and two oxygen atoms (water molecules) were used as fragments. Two of the 20 parallel tempering cycles had cost factors much lower than the others (10% success rate). This model has a chair conformation of the C_4N_2 ring and a different orientation of the tetrahydrofuran ring. One of the water molecules was unreasonable (overlapped other atoms), and was placed manually in a small void in the structure.

Rietveld refinement was carried out using GSAS (Toby, 2001; Larson and Von Dreele, 2004). Only the 2.0–26.0° portion of the pattern was included in the refinement (d_{min} = 1.017 Å). All non-H bond distances and angles were subjected to restraints, based on a Mercury/Mogul Geometry check (Bruno *et al*., 2004; Sykes *et al*., 2011) of the molecule. The Mogul average and standard deviation for each quantity were used as the restraint parameters. The restraints contributed 7.3% to the final χ^2. The hydrogen atoms were included in calculated positions, which were recalculated during the refinement using Materials Studio (Dassault, 2016). Positions of the active hydrogens were derived by the analysis of potential hydrogen bonding patterns. A common U_{iso} was refined for the non-H atoms of the fused-ring system, another U_{iso} for the non-H substituent atoms, another for the non-H atoms of the C_4N_2 ring, another for the non-H atoms of the tetrahydrofuran ring, and a common U_{iso} for the water molecules. The U_{iso} for each hydrogen atom was constrained to be 1.3× that of the heavy atom to which it is attached. The peak profiles were described using profile function #4 (Thompson *et al*., 1987; Finger *et al*., 1994), which includes the Stephens (1999) anisotropic strain broadening model. The background was modeled using a three-term shifted Chebyshev polynomial, with a seven-term diffuse scattering function to model the Kapton capillary and any amorphous component. The final refinement of 138 variables using 24118 observations (24037 data points and 81 restraints) yielded

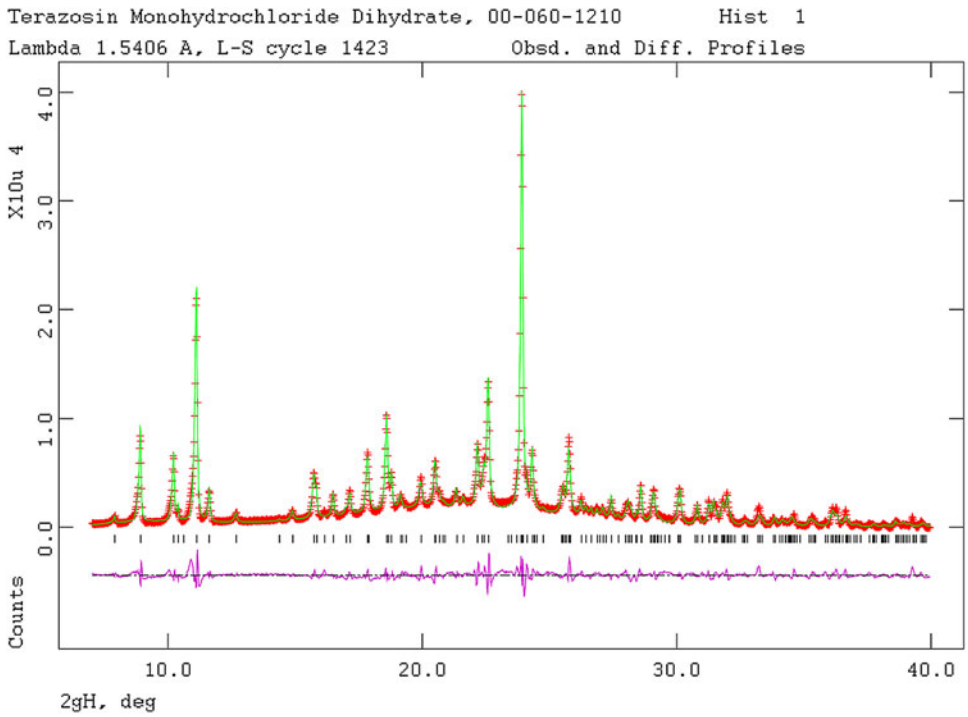

Figure 4. (Color online) The Rietveld plot for the refinement of terazosin hydrochloride dihydrate using the laboratory data of PDF entry 00-060-1210. The red crosses represent the observed data points, and the green line is the calculated pattern. The magenta curve is the difference pattern, plotted at the same vertical scale as the other patterns.

https://doi.org/10.1017/S0885715618000490 Published online by Cambridge University Press

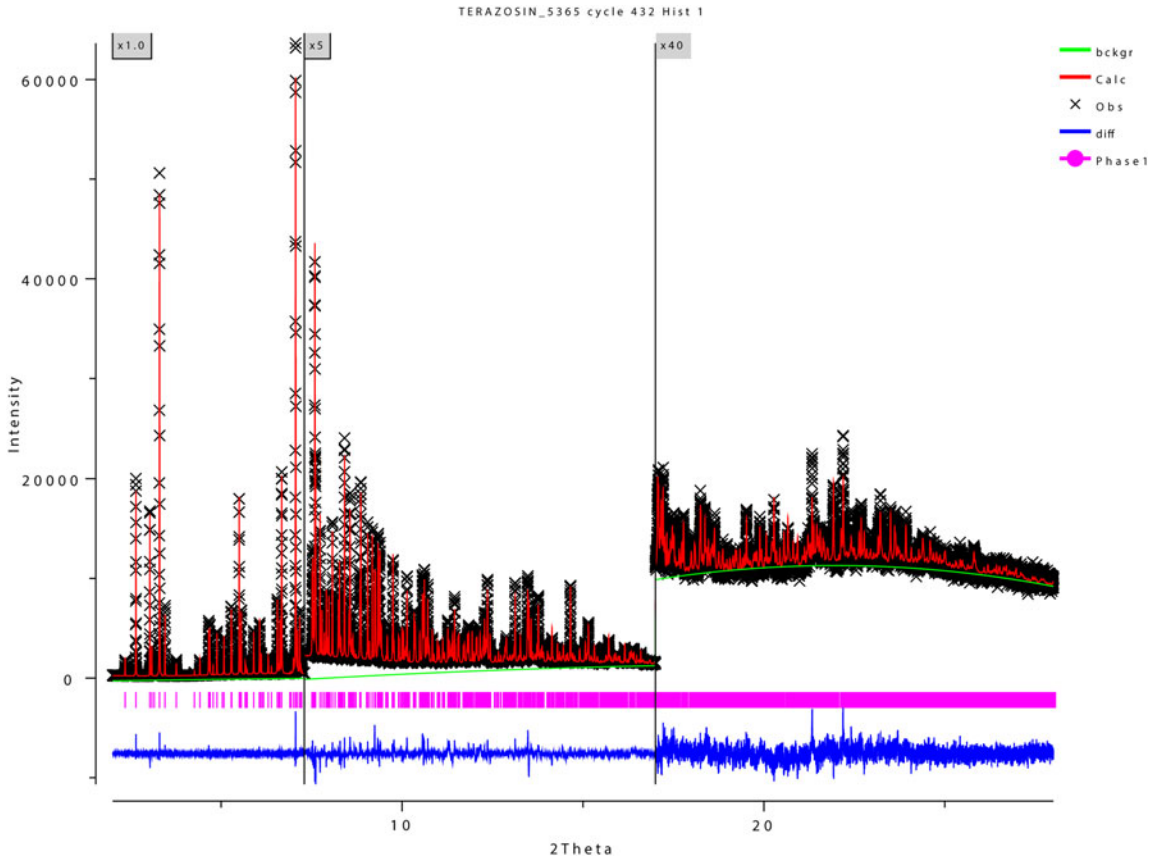

Figure 5. (Color online) The Rietveld plot for the refinement of terazosin hydrochloride dihydrate using the synchrotron data. The black crosses represent the observed data points, and the red line is the calculated pattern. The blue curve is the difference pattern, plotted at the same vertical scale as the other patterns. The vertical scale has been multiplied by a factor of 5 for $2\theta > 7.4°$, and by a factor of 40 for $2\theta > 17.0°$.

the residuals $R_{wp} = 0.0807$, $R_p = 0.0594$, and $\chi^2 = 4.006$. The largest peak (1.10 Å from C42) and hole (1.48 Å from C6) in the difference Fourier map were 0.40 and -0.41 eÅ^{-3}, respectively. The Rietveld plot is included as Figure 5. The largest errors in the fit are in the shapes of some of the strong peaks.

A density functional geometry optimization (fixed experimental unit cell) was carried out using CRYSTAL14 (Dovesi *et al*., 2014). The basis sets for the H, C, and O atoms were those of Gatti *et al*. (1994), and the basis set for chlorine was that of Peintinger *et al*. (2013). The calculation was run on eight 2.1 GHz Xeon cores (each with 6 Gb RAM) of a 304-core Dell Linux cluster at IIT, using 8 *k*-points and the B3LYP functional, and took ∼48 h.

III. RESULTS AND DISCUSSION

The synchrotron and laboratory powder patterns match that of Figure 2 of US Patent 5 294 615 well enough (Figure 6) to conclude that the sample studied here is the crystalline terazosin hydrochloride dihydrate marketed as Hytrin®.

The refined atom coordinates of terazosin hydrochloride dihydrate and the coordinates from the density functional theory (DFT) optimization are reported in the Crystallographic Information Framework (CIF) files attached as Supplementary Material. The root-mean-square Cartesian displacement of the non-hydrogen atoms in the terazosin cations is 0.177 Å (Figure 7). The largest deviation is 0.351 Å at C51 in the tetrahydrofuran ring. The good agreement between the refined and optimized structures is evidence that the experimental structure is correct (van de Streek and Neumann, 2014). This discussion uses the DFT-optimized structure. The asymmetric unit (with atom numbering) is illustrated in Figure 8, and the crystal structure is presented in Figure 9. The packing diagram hints that some π–π interactions may be present, but there is no evidence for them in the DFT calculation.

All of the bond distances, bond angles, and torsion angles fall within the normal ranges indicated by a Mercury Mogul Geometry check (Macrae *et al*., 2008). The N26–C10 and N39–C40 bonds, which link the C_4N_2 ring to the other parts of the molecule, are significantly shorter (1.357 Å) than the C–N bonds within this ring (∼1.465 Å). This shorter distance might provide evidence of multiple bonding, but the Mulliken overlap populations in these bonds do not differ significantly from the other C–N single bonds. Quantum chemical geometry optimizations (DFT/631G*/water) using Spartan ‘16 (Wavefunction, 2017) indicated that the observed conformation of terazosin in terazosin hydrochloride dihydrate is 9.0 kcal mole^{-1} higher in energy than the local minimum energy conformation. The rms Cartesian displacement is 0.180 Å, and the largest differences are in the tetrahydrofuran and C_4N_2 rings of the molecule. Molecular mechanics conformational analysis indicated that the global minimum energy conformation (-8.4 kcal mole^{-1}) has a more compact conformation with the tetrahydrofuran end of the molecule curled

https://doi.org/10.1017/S0885715618000490 Published online by Cambridge University Press

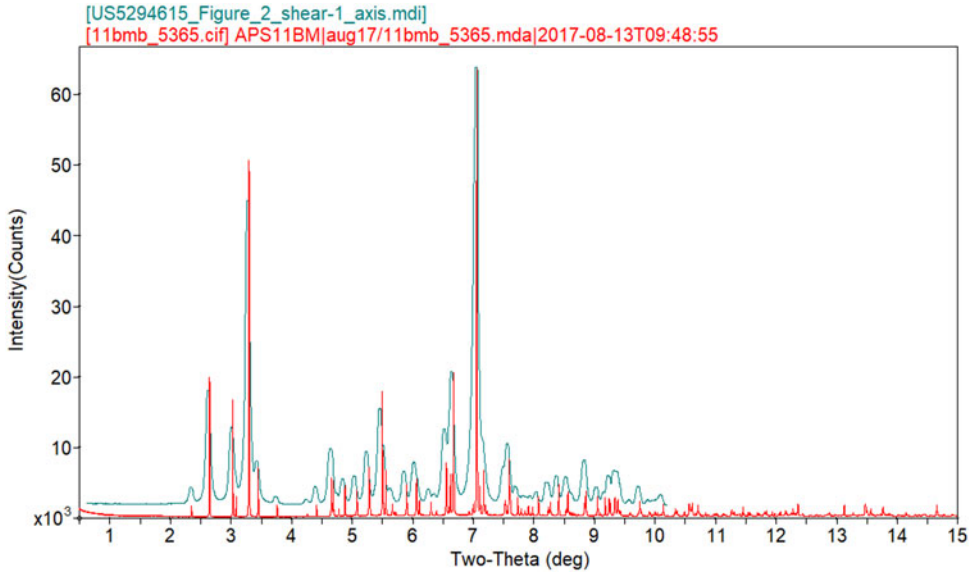

Figure 6. (Color online) Comparison of the synchrotron pattern with that of terazosin hydrochloride dihydrate from Figure 2 of US Patent 5 294 615. The patent pattern (measured using Cu$K\alpha$ radiation) was digitized using UN-SCAN-IT, corrected for a 1° shear in the patent figure using Adobe Illustrator, and re-scaled to the synchrotron wavelength of 0.457667 Å using Jade 9.7.

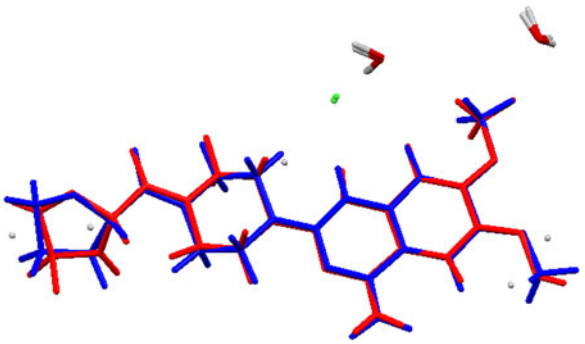

Figure 7. (Color online) Comparison of the refined and optimized structures of the cation in terazosin hydrochloride dihydrate. The Rietveld refined structure is in red, and the DFT-optimized structure is in blue.

toward the rest of the molecule, an indication intermolecular interactions are important in determining the solid-state conformation.

Two independent structure solutions and density functional optimizations yielded structures with slightly different orientations of the tetrahydrofuran ring. The crystal energies were within 0.03 kcal mole^{-1} of each other, suggesting the possibility of disorder on that end of the molecule. The U_{iso} of the atoms in the tetrahydrofuran and the C_4N_2 rings are larger than those in the other portion of the molecule, but the difference Fourier map shows no clear evidence for disorder.

Analysis of the contributions to the total crystal energy using the Forcite module of Materials Studio (Dassault, 2016) suggests that angle, bond, and torsion distortion terms are significant in the intramolecular deformation energy, as

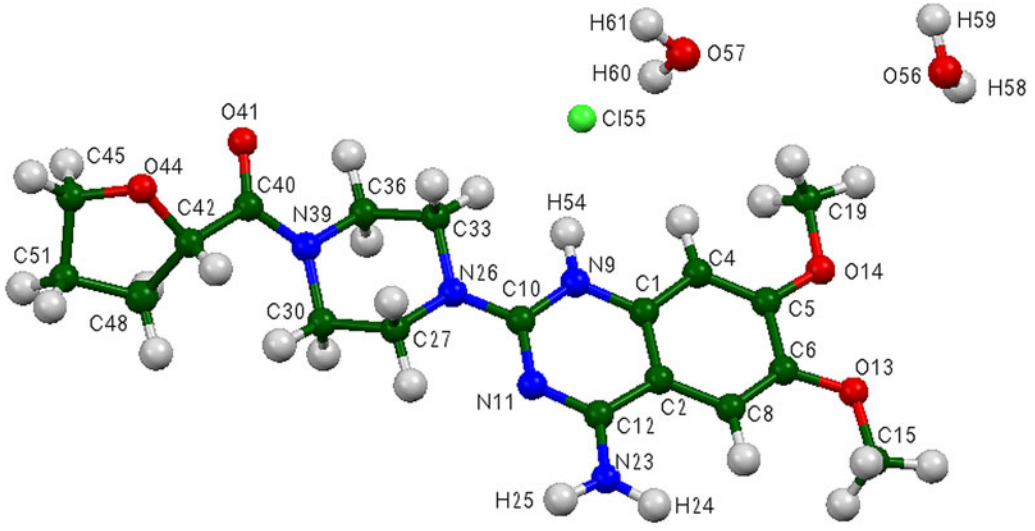

Figure 8. (Color online) The asymmetric unit of terazosin hydrochloride dihydrate, with the atom numbering. The atoms are represented by 50% probability spheroids.

https://doi.org/10.1017/S0885715618000490 Published online by Cambridge University Press

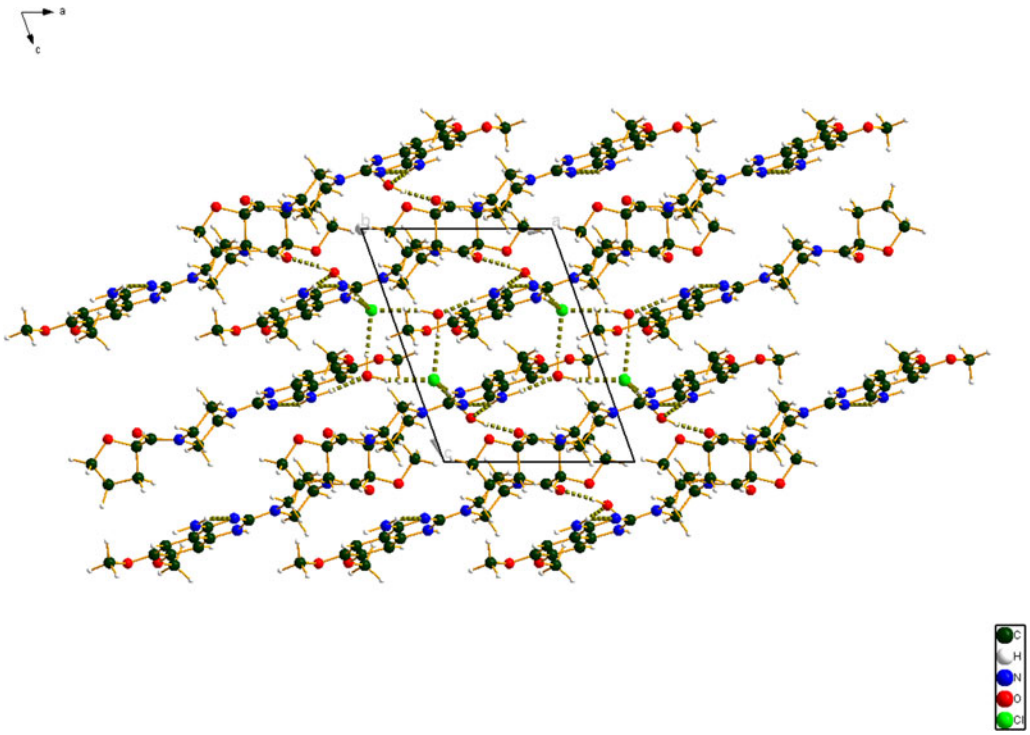

Figure 9. (Color online) The crystal structure of terazosin hydrochloride dihydrate, viewed down the *b*-axis.

might be expected from a fused ring system. The intermolecular energy contains significant contributions from electrostatic attractions, which in this force-field-based analysis include hydrogen bonds. The hydrogen bonds are better analyzed using the results of the DFT calculation.

As expected from the chemistry, hydrogen bonds are important in the crystal structure (Table I). The chloride anion accepts hydrogen bonds from three of the four protons of the water molecules. The energies of these three hydrogen bonds were calculated using a correlation described in Kaduk (2002). The chloride also acts as the acceptor in a N9–H54•••Cl55 hydrogen bond from the protonated ring nitrogen; the short N•••Cl distance established that the protonation occurred on N9. The Cl also participates in two weaker C–H•••Cl hydrogen bonds. The amino group N23 acts as a hydrogen bond donor to two water molecules. The energies of these hydrogen bonds were calculated using the correlation in Wheatley and Kaduk (2018). For the remaining water molecule, hydrogen acts as a donor to the ketone oxygen O41. The energy of this hydrogen bond was calculated by the correlation of Rammohan and Kaduk (2018). The aromatic ring carbon C8 makes a strong C–H•••O hydrogen bond to the water molecule O57. C–H•••O and C–H•••N hydrogen bonds also contribute to the crystal energy. Two of these are intramolecular, and presumably help determine the conformation of the molecule. In addition to the ketone oxygen O41, both of the ether oxygen atoms O13 and O14 act as hydrogen bond acceptors. Most of these hydrogen bonds are discrete, but the water molecule H60–O57–H61 and the chlorine Cl55 form a ring with graph set (Etter, 1990; Bernstein *et al.*, 1995; Shields *et al.*, 2000) *R*2,4(8). The terazosin molecules lie roughly in the (328) plane.

TABLE I. Hydrogen bonds (CRYSTAL14) in terazosin hydrochloride dihydrate.

H-bond	D–H, Å	H···A, Å	D···A, Å	D–H···A,°	Overlap, *e*	*E*, kcal mole^{-1}
O57–H60···Cl55	0.981	2.201	3.177	173.4	0.062	35.1
O57–H61···Cl55	0.978	2.271	3.234	167.9	0.053	32.4
O56–H58···Cl55	0.974	2.334	3.295	168.9	0.050	31.5
N9–H54···Cl55	1.024	2.324	3.322	164.5	0.059	
C23–H34···Cl55	1.089	2.536	3.635	166.9	0.030	
C4–H3···Cl55	1.081	2.657	3.595	144.8	0.028	
N23–H25···O56	1.034	1.857	2.890	177.4	0.080	6.5
N23–H24···O57	1.021	1.938	2.953	172.1	0.046	4.9
O56–H59···O41	0.979	1.767	2.700	158.1	0.043	11.3
C8–H7···O57	1.084	2.309	3.361	162.9	0.043	
C36–H37···O41	1.088*	2.218	2.716	105.3	0.022	
C15–H16···O14	1.087	2.244	3.320	169.8	0.021	
C27–H28···N11	1.089*	2.270	2.726	103.4	0.020	
C27–H29···O13	1.097	2.435	3.518	169.1	0.019	
C19–H21···O41	1.095	2.657	3.634	148.3	0.011	

*Intramolecular.

https://doi.org/10.1017/S0885715618000490 Published online by Cambridge University Press

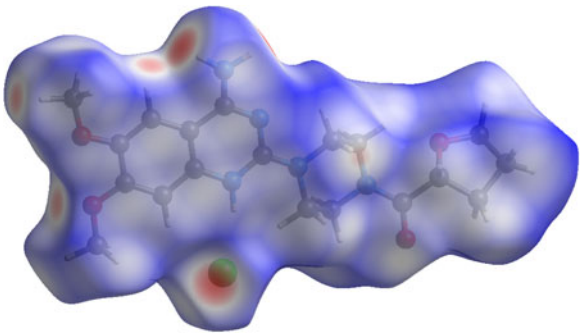

Figure 10. (Color online) The Hirshfeld surface of terazosin hydrochloride dihydrate. Intermolecular contacts longer than the sums of the van der Waals radii are colored blue, and contacts shorter than the sums of the radii are colored red. Contacts equal to the sums of radii are white.

The *R*2,4(8) hydrogen bond pattern links the planes of the molecules. The other hydrogen bonds contribute to a three-dimensional hydrogen bond network.

The volume enclosed by the Hirshfeld surface (Figure 10; Hirshfeld, 1977; McKinnon *et al*., 2004; Spackman and Jayatilaka, 2009; Wolff *et al*., 2012) is 546.43 Å^3, 97.74% of 1/2 the unit-cell volume. The molecules are thus not tightly packed. All of the significant close contacts (red in Figure 10) involve the hydrogen bonds.

The Bravais–Friedel–Donnay–Harker (Bravais, 1866; Friedel, 1907; Donnay and Harker, 1937) morphology suggests that we might expect blocky morphology for terazosin hydrochloride dihydrate, with {001}, {010}, and {011} as the principal faces. A sixth-order spherical harmonic preferred orientation model was included in the refinement; the texture index was 1.0210, indicating that preferred orientation was not significant in this rotated capillary specimen. The powder pattern of terazosin hydrochloride dihydrate from this synchrotron data set has been submitted to ICDD for inclusion in the Powder Diffraction File.

SUPPLEMENTARY MATERIAL

The supplementary material for this article can be found at https://doi.org/10.1017/S0885715618000490

ACKNOWLEDGEMENTS

Use of the Advanced Photon Source at Argonne National Laboratory was supported by the US Department of Energy, Office of Science, Office of Basic Energy Sciences, under Contract No. DE-AC02-06CH11357. This work was partially supported by the International Centre for Diffraction Data. The authors thank Lynn Ribaud and Saul Lapidus for their assistance in the data collection, and Andrey Rogachev for the use of computing resources at IIT.

Bernstein, J., Davis, R. E., Shimoni, L., and Chang, N. L. (**1995**). "Patterns in hydrogen bonding: functionality and graph set analysis in crystals," Angew. Chem. Int. Ed. Engl. **34**(15), 1555–1573.

Bravais, A. (**1866**). *Etudes Cristallographiques* (Gauthier Villars, Paris).

Bruno, I. J., Cole, J. C., Kessler, M., Luo, J., Motherwell, W. D. S., Purkis, L. H., Smith, B. R., Taylor, R., Cooper, R. I., Harris, S. E., and Orpen, A. G. (**2004**). "Retrieval of crystallographically-derived molecular geometry information," J. Chem. Inf. Sci. **44**, 2133–2144.

Cannata, V., Ferrario, T., and Galbiati, B. (**1999**). "Process for the Production of the Form I of the Terazosin Monohydrochloride Anhydrous," US Patent 5856482 (ALFA Chemicals Italiana S.R.L.).

Dassault Systèmes (**2016**). *Materials Studio 2017R2* (BIOVIA, San Diego, CA).

Donnay, J. D. H. and Harker, D. (**1937**). "A new law of crystal morphology extending the law of Bravais," Am. Mineral. **22**, 446–447.

Dovesi, R., Orlando, R., Erba, A., Zicovich-Wilson, C. M., Civalleri, B., Casassa, S., Maschio, L., Ferrabone, M., De La Pierre, M., D-Arco, P., Noël, Y., Causà, M., and Kirtman, B. (**2014**). "CRYSTAL14: a program for the ab initio investigation of crystalline solids," Int. J. Quantum Chem. **114**, 1287–1317.

Etter, M. C. (**1990**). "Encoding and decoding hydrogen-bond patterns of organic compounds," Acc. Chem. Res. **23**(4), 120–126.

Favre-Nicolin, V. and Černý, R. (**2002**). FOX, "Free Objects for crystallography: a modular approach to ab initio structure determination from powder diffraction," J. Appl. Crystallogr. **35**, 734–743.

Fawcett, T. G., Kabekkodu, S. N., Blanton, J. R., and Blanton, T. N. (**2017**). "Chemical analysis by diffraction: the Powder Diffraction File™," Powder Diffr. **32**(2), 63–71.

Finger, L. W., Cox, D. E., and Jephcoat, A. P. (**1994**). "A correction for powder diffraction peak asymmetry due to axial divergence," J. Appl. Crystallogr. **27**(6), 892–900.

Friedel, G. (**1907**). "Etudes sur la loi de Bravais," Bull. Soc. Fr. Mineral. **30**, 326–455.

Gatti, C., Saunders, V. R., and Roetti, C. (**1994**). "Crystal-field effects on the topological properties of the electron-density in molecular crystals – the case of urea," J. Chem. Phys. **101**, 10686–10696.

Groom, C. R., Bruno, I. J., Lightfoot, M. P., and Ward, S. C. (**2016**). "The Cambridge Structural Database," Acta Crystallogr. Sect. B Struct. Sci. Cryst. Eng. Mater. **72**, 171–179.

Hirshfeld, F. L. (**1977**). "Bonded-atom fragments for describing molecular charge densities," Theor. Chem. Acta **44**, 129–138.

ICDD (**2017**). *PDF-4 + 2018 (Database)*, edited by S. Kabekkodu (International Centre for Diffraction Data, Newtown Square, PA, USA).

Kaduk, J. A. (**2002**). "Use of the Inorganic Crystal Structure Database as a problem solving tool," Acta Crystallogr. Sect. B Struct. Sci. **58**, 370–379.

Kaduk, J. A., Crowder, C. E., Zhong, K., Fawcett, T. G., and Suchomel, M. R. (**2014**). "Crystal structure of atomoxetine hydrochloride (Strattera), $C_{17}H_{22}NOCl$," Powder Diffr. **29**(3), 269–273.

Larson, A. C. and Von Dreele, R. B. (**2004**). General Structure Analysis System (GSAS) (Los Alamos National Laboratory Report LAUR 86-784).

Lee, P. L., Shu, D., Ramanathan, M., Preissner, C., Wang, J., Beno, M. A., Von Dreele, R. B., Ribaud, L., Kurtz, C., Antao, S. M., Jiao, X., and Toby, B. H. (**2008**). "A twelve-analyzer detector system for high-resolution powder diffraction," J. Synch. Radiat. **15**(5), 427–432.

Macrae, C. F., Bruno, I. J., Chisholm, J. A., Edington, P. R., McCabe, P., Pidcock, E., Rodriguez-Monge, L., Taylor, R., van de Streek, J., and Wood, P. A. (**2008**). "Mercury CSD 2.0 – new features for the visualization and investigation of crystal structures," J. Appl. Crystallogr. **41**, 466–470.

McKinnon, J. J., Spackman, M. A., and Mitchell, A. S. (**2004**). "Novel tools for visualizing and exploring intermolecular interactions in molecular crystals," Acta Crystallogr. Sect. B **60**, 627–668.

Meyer, G. A. and Bauer, J. F. (**1994**). "Terazosin polymorph and pharmaceutical composition," US Patent 5,294,615.

O'Boyle, N., Banck, M., James, C. A., Morley, C., Vandermeersch, T., and Hutchison, G. R. (**2011**). "Open Babel: an open chemical toolbox," J. Chem. Inform. **3**, 33

Peintinger, M. F., Vilela Oliveira, D., and Bredow, T. (**2013**). "Consistent Gaussian basis sets of triple-zeta valence with polarization quality for solid-state calculations," J. Comput. Chem. **34**, 451–459.

Rammohan, A. and Kaduk, J. A. (**2018**). "Crystal structures of alkali metal (Group 1) citrate salts," Acta Crystallogr. B Struct. Sci. Cryst. Eng. Mat., **74**, 239–252.

Roteman, R. (**1979**). "1-(4-amino-6,7-dimethoxy-2-quinazolinyl)-4-(2-tetrahydrofuroyl) piperazine hydrochloride dihydrate," US Patent 4,251,532.

Shields, G. P., Raithby, P. R., Allen, F. H., and Motherwell, W. S. (**2000**). "The assignment and validation of metal oxidation states in the Cambridge Structural Database," Acta Crystallogr. Sect. B Struct. Sci. **56**(3), 455–465.

Spackman, M. A. and Jayatilaka, D. (**2009**). "Hirshfeld surface analysis," CrystEngComm **11**, 19–32.

Stephens, P. W. (**1999**). "Phenomenological model of anisotropic peak broadening in powder diffraction," J. Appl. Crystallogr. **32**, 281–289.

Sykes, R. A., McCabe, P., Allen, F. H., Battle, G. M., Bruno, I. J., and Wood, P. A. (**2011**). "New software for statistical analysis of Cambridge Structural Database data," J. Appl. Crystallogr. **44**, 882–886.

Thompson, P., Cox, D. E., and Hastings, J. B. (**1987**). "Rietveld refinement of Debye-Scherrer synchrotron X-ray data from Al_2O_3," J. Appl. Crystallogr. **20**(2), 79–83.

Toby, B. H. (**2001**). "EXPGUI, a graphical user interface for GSAS," J. Appl. Crystallogr. **34**, 210–213.

van de Streek, J. and Neumann, M. A. (**2014**). "Validation of molecular crystal structures from powder diffraction data with dispersion-corrected density functional theory (DFT-D)," Acta Crystallogr. Sect. B Struct. Sci. Cryst. Eng. Mater. **70**(6), 1020–1032.

Wang, J., Toby, B. H., Lee, P. L., Ribaud, L., Antao, S. M., Kurtz, C., Ramanathan, M., Von Dreele, R. B., and Beno, M. A. (**2008**). "A dedicated powder diffraction beamline at the Advanced Photon Source: commissioning and early operational results," Rev. Sci. Inst. **79**, 085105.

Wavefunction, Inc. (**2017**). Spartan '16 Version 2.0.1, Wavefunction Inc., 18401 Von Karman Ave., Suite 370, Irvine CA 92612.

Wheatley, A. M. and Kaduk, J. A. (**2018**). "Crystal structures of ammonium citrates," manuscript in preparation.

Wolff, S. K., Grimwood, D. J., McKinnon, M. J., Turner, M. J., Jayatilaka, D., and Spackman, M. A. (**2012**). Crystal Explorer Version 3.1 (University of Western Australia).

https://doi.org/10.1017/S0885715618000490 Published online by Cambridge University Press